Available online at www.sciencedirect.com
SCIENCE DIRECT®
Journal of Molecular Catalysis B: Enzymatic 22 (2003) 299–306
JOURNAL OF MOLECULAR CATALYSIS B: ENZYMATIC
www.elsevier.com/locate/molcatb

Improving cutinase stability in aqueous solution and in reverse micelles by media engineering

Eduardo P. Melo [a,b,*], Ricardo P. Baptista [b], Joaquim M.S. Cabral [b]

[a] *Faculdade de Engenharia dos Recursos Naturais (FERN), Universidade do Algarve, Campus de Gambelas, 8000 Faro, Portugal*
[b] *Centro de Engenharia Biológica e Química, Instituto Superior Técnico, 1049-001 Lisbon, Portugal*

Abstract

The stability of a recombinant cutinase from the fungus *Fusarium solani* was evaluated in aqueous media and in reverse micelles. Thermal unfolding in aqueous solution is a two-state process at the pH values tested and trehalose increased the temperature at the mid-point of the unfolding transitions. Irreversible inactivation is a first-order process at pH 9.2, but two inactivation phases were resolved at pH 4.5. Trehalose did not change the irreversible inactivation pathway but increased the kinetics of the irreversible inactivation step. Unfolding of cutinase induced by guanidine hydrochloride was more complex, showing a stable intermediate, molten globule in character, within the transition region. Trehalose did not change the three-state nature of the unfolding process. Encapsulation of cutinase in AOT reverse micelles induced unfolding at room temperature due to an enzyme location at the micellar interface. The presence of 1-hexanol as co-surfactant delayed or even prevented the unfolding of cutinase by promoting the establishment of a new equilibrium in the system. Cutinase is encapsulated in a 10-fold larger AOT/hexanol reverse micelle built up by the fusion of empty reverse micelles. When tested in a membrane reactor in the presence of 1-hexanol, an operational half-life of 674 days was achieved.

Keywords: Cutinase; Protein stability; Trehalose; Reverse micelles

1. Introduction

Cutinases are synthesised by fungi and pollen tubes during their penetration of the plant cuticle, which covers plant surfaces [1]. Pathogenic fungi produce and secrete cutinase to hydrolyse cutin, the main structural component of the cuticle. Cutin is an insoluble polyester composed of hydroxy- and hydroxyepoxy-fatty acids derived from saturated C16 and unsaturated C18 fatty acids. Fungal cutinases belong to the class of serine esterases, which have the classic catalytic triad composed of serine, histidine and a carboxyl group. The involvement of an active serine explains cutinase inhibition by organophosphates, organic boronic acid derivatives and alkylisocyanates [1].

The gene of cutinase from *Fusarium solani* was cloned in *Escherichia coli* fused with the signal peptide for alkaline phosphatase in order to direct the cutinase to the *E. coli* periplasm [2]. This simplifies the extraction and purification processes. Despite the lack of glycosylation and the presence of a N-terminal extension, the recombinant cutinase, with 197 residues (Protein Data Bank entry 1AGY) and an isoelectric point of 7.6, displays an enzymatic activity comparable to the native protein. The stretch of residues containing the active site serine (Gly-Tyr-Ser-Gln-Gly) matches the consensus sequence commonly present in esterases and lipases (Gly-X-Ser-X-Gly) [3].

* Corresponding author. Fax: +351-21-8419062.
E-mail address: emelo@ualg.pt (E.P. Melo).

1381-1177/03/$ – see front matter © 2003 Elsevier Science B.V. All rights reserved.
doi:10.1016/S1381-1177(03)00044-4

In addition to hydrolysis of solid cutin, the recombinant cutinase from *F. solani* also displays esterase and lipolytic activities with a kinetic behaviour intermediate between esterases and lipases, since it is able to hydrolyse both aggregated and soluble substrates [4,5]. For most lipases, a structural rearrangement of the lid covering the active site occurs to allow the substrate to dock in the active site. This could explain the enhancement of activity in the presence of a lipid–water interface, the so-called interfacial activation [6]. This property is quite different from that of the usual esterases acting on water-soluble carboxylic ester molecules. The three-dimensional structure of the recombinant cutinase was initially solved at 1.6 Å [7] and more recently to an atomic resolution of 1.0 Å [8]. It is a compact one-domain molecule (45 Å × 30 Å × 30 Å in size) and the later high-resolution study suggested the existence of a "breath-like" movement in the mini-lid of cutinase that may be responsible for the adaptation to different substrates. Recently, an NMR study points to the presence of an open and close binding site conformation in the free cutinase which indicates that it is a lipase rather than an esterase [9]. When acting on triglycerides substrates, cutinase is very sensitive to the length and position of the acyl chain. The highest activities were found when the chains at positions 1 and 3 contain three or four carbon atoms [10].

Cutinase is a versatile enzyme showing several noteworthy properties for application in industrial products and processes. An enzymatic preparation containing cutinase has been developed for increasing the pharmacological effect of agricultural chemicals [11]. Cutinase has been applied as a lipolytic enzyme in laundry and dishwashing detergent compositions to remove fats [12,13]. Degradation of plastics such as the synthetic polyester polycaprolactone to water-soluble products has been achieved with cutinase [14]. Other potential uses include the hydrolysis of milk fat in the dairy industry, the oleochemistry industry and the synthesis of structured triglycerides, polymers and surfactants for personal-care products, pharmaceuticals and agrochemicals containing one or more chiral centres [15].

Protein stability is a main concern to enzyme applications. The benefits of using enzymes as catalyst at high temperatures, such as an increase in rates of reactions and yields [16], combined with reduced contamination and viscosity [17] make thermal stability perhaps the most thoroughly investigated aspect of enzyme inactivation. However, thermal stability is often more complicated than just a reversible unfolding. Irreversible processes such as aggregation, misfolding or even adverse covalent reactions are common and make the elucidation of the deactivation pathway and the development of strategies for increased stability more complex. On contrary, the use of urea or guanidine hydrochloride as protein denaturants has some advantages: (1) the extent of unfolding is generally greater than can be achieved using temperature [18]; (2) unfolding is completely reversible; and (3) aggregation is seldom observed. Thermodynamic stability of proteins and reversible unfolding pathways are usually assessed using these denaturants. Cutinase stability at different temperatures and guanidine hydrochloride concentrations have been studied in order to characterize unfolding pathways and the effect of low molecular weight solutes [19,20]. Media engineering using additives, such as low molecular weight solutes, is one of the earliest strategies developed to stabilize proteins. However, the molecular mechanism involved on protein stabilisation is still matter of debate despite the proposal of some principles [21,22].

The use of enzymes in non-conventional media is an attractive strategy, especially when lipophilic substrates and/or products are employed and a low water content is desirable. Transesterification of fats and oils or (stereo)selective esterification of alcohols are potential applications for low water systems such as reverse micelles. In essence reverse micelles are nanometer-sized water droplets dispersed in organic media by the action of surfactants. The surfactant molecules are arranged with the polar part to the inner side as they are able to solubilize water and the apolar part in contact with the organic solvent. Enzymes can be solubilized in the water droplet and the water activity can be controlled to shift the thermodynamic equilibrium in favour of synthesis rather than of hydrolysis. In addition, higher amounts of hydrophobic substrates can be solubilized in the organic solvent having at the same time a higher interfacial area between the aqueous and the organic phase to minimize mass transfer problems. Probably, the major problem associated with these systems is the enzyme performance. The physico-chemical properties of the environment in which the enzyme is solubilized are distinct from a bulk aqueous solution

affecting the activity and the stability of the enzyme. Structure–function relationships of enzymes are therefore critical to assess and improve the potential use of enzymes in these non-conventional media. This paper reviews two strategies of media engineering used in our laboratory to improve cutinase stability. Trehalose was used to improve the thermal stability of cutinase in aqueous solution [19,20] and 1-hexanol has shown to improve the stability of cutinase in AOT (dioctyl sulfosuccinate sodium salt, a negatively charged surfactant) reverse micelles [15,23–25].

2. Cutinase stability in aqueous solution: the effect of trehalose

2.1. Thermal stability

Thermal unfolding of cutinase was studied at pH 4.5 and in the alkaline pH range (pH > 9.2) [19]. The cutinase solution was heated and the near-UV absorbance [26] or the fluorescence intensity was recorded to quantify the fraction of unfolded cutinase. Between pH 4.5 and 9.2 aggregation occurs and spectroscopic measurements could not be recorded. The thermal unfolding curves were well-fitted to a two-state mechanism where only the folded and unfolded conformations were present (as shown in Fig. 1). The two-state nature of the unfolding process induced by temperature was confirmed by comparing unfolding curves recorded by UV difference spectroscopy and tryptophyl and 8-anilino-1-naphthalene sulfonic acid (ANS) fluorescence [20]. The ANS dye has been used to detect folding intermediates [27] known as molten globules, although the mode of ANS binding and its influence on the fluorescence are not well understood [28]. The temperatures at the mid-point of the unfolding transitions (where $\Delta G^\circ = 0$) were calculated and used as an index of protein stability (Table 1). In the alkaline pH range, the stability increases with decreasing pH. Lower pH values in this range also lead to higher degrees of reversibility after cooling the protein solution to 25 °C (Fig. 1). The presence of trehalose, an uncharged disaccharide well known as a protein stabilizer, increases the T_m (Table 1) but does not change the two-state nature of the unfolded process (data not shown except for pH 9.2).

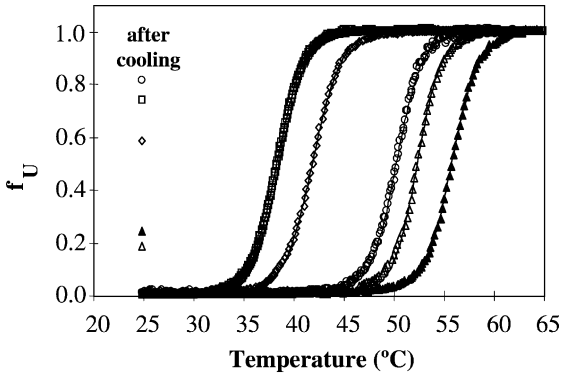

Fig. 1. Thermal unfolding of cutinase at pH 4.5 (○), pH 9.2 in the absence (△) and presence of trehalose (▲), pH 10.5 (◇) and pH 10.9 (□). The single experimental points at 25 °C are the fraction of cutinase irreversible unfolded (f_U after cooling). Lines were calculated according to a two-state mechanism using the following equation: $f_U = e^{(-\Delta G^\circ/RT)}/(1 + e^{(-\Delta G^\circ/RT)})$ where ΔG° is the standard free energy change for the thermal unfolding.

Irreversible inactivation experiments were carried out at pH 4.5 and 9.2. Cutinase solutions were incubated at a fixed temperature within the transition region and samples were taken periodically and rapidly cooled before assaying for activity. With this procedure, all cutinase molecules that are reversibly unfolded at the incubation temperature will refold during cooling and only the irreversibly inactivated molecules will be quantified. The inactivation is a first-order process at pH 9.2, but two phases were clearly resolved at pH 4.5 (Fig. 2 and Table 2). At this lower pH, a fast phase is observed initially followed by a slow phase. Trehalose does not change the irreversible inactivation pathway since the number of phases remains constant depending only on the pH. Trehalose decreases the observable rate constant at pH 9.2, but this is an apparent

Table 1
Temperature values at mid-point (50% of cutinase is unfolded) for thermal-induced cutinase unfolding in the absence and presence of 0.5 M trehalose

pH	T_m (°C) (no trehalose)	T_m (°C) (0.5 M trehalose)
4.5	49.8 ± 0.5	53.0
9.2	52.6 ± 0.1	56.6 ± 0.5
10.5	42.0 ± 0.1	44.6 ± 1.5
10.9	38.5	–[a]

Values in the alkaline pH range were from Baptista et al. [19].
[a] Value not determined.

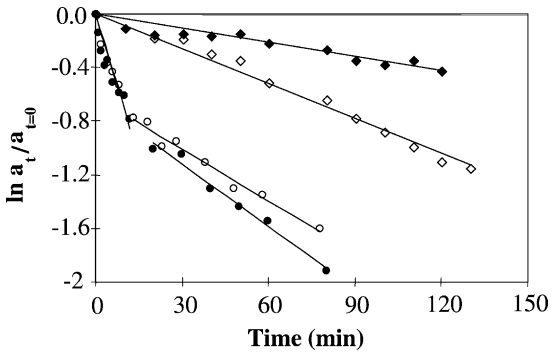

Fig. 2. Irreversible inactivation of cutinase after incubation at 55 °C. Four conditions were tested: pH 4.5 in the absence (○) and presence of 0.5 M trehalose (●) and pH 9.2 in the absence (◇) and presence of 0.5 M trehalose (◆). The experimental observed rate constants were calculated from the slops of the semi-log fits and are shown in Table 2.

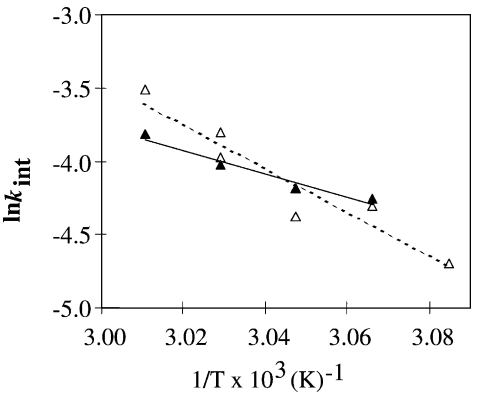

Fig. 3. Arrhenius plot of intrinsic rate constants for the irreversible inactivation step at pH 9.2 in the absence (△) and presence of 0.5 M trehalose (▲).

value as described below. At pH 4.5, no significant effect on the rate constants was observed for trehalose.

At pH 9.2, around 80% of the cutinase molecules refold upon cooling after the thermal unfolding and trehalose slightly increased the degree of irreversibility (Fig. 1). Therefore, at this pH value it can be assured that when the protein is initially incubated at a fixed temperature within the transition region no irreversible inactivated states were yet formed. In other words, at the time zero of an irreversible inactivation experiment only the folded and reversibly unfolded states are present (F ↔ U). The equilibrium constant $K_{U–F}$ for the reversible step can be calculated with accuracy. The classical model for the thermal inactivation considers first a reversible step followed by an irreversible step according to the following pathway: F ↔ U → I [29]. Therefore, the experimentally observed rate constants presented in Table 2 depend on the previous reversible step (for a first-order process $d[I]/dt = k[U]$ and [U] depends on $K_{U–F} = [U]/[F]$). Once the equilibrium constant is calculated with accuracy at pH 9.2 the experimental rate constant can be related to the intrinsic monomolecular rate constant of the irreversible step [19,30]. These are plotted in Fig. 3 according to Arrhenius law. Despite some scatter in the data points (due to calculation using two parameters, the observed rate constant and the equilibrium constant $K_{U–F}$) the activation energy was calculated and is higher in the absence (30 kcal mol^{-1}) than in the presence of trehalose (16 kcal mol^{-1}). This shows that kinetics of the irreversible step increased in the presence of trehalose. In conclusion, trehalose only stabilises the reversible step of thermal denaturation of cutinase (shown by the increase on T_m). Neither the nature of the reversible step (two-state) nor that of the irreversible step (one phase at pH 9.2 and two phases at pH 4.5) are changed in the presence of trehalose.

2.2. Guanidine hydrochloride induced unfolding of cutinase

Unfolding transitions of cutinase at pH 4.5 induced by guanidine hydrochloride were assessed by near-UV

Table 2
Experimentally observed rate constants for the irreversible inactivation of cutinase at 55 °C

pH	No trehalose			0.5 M trehalose		
	$k_{fast-phase}$ (min^{-1})	$k_{slow-phase}$	$k_{single-phase}$	$k_{fast-phase}$	$k_{slow-phase}$	$k_{single-phase}$
4.5	0.072	0.013	–[a]	0.070	0.016	–[a]
9.2	–[a]	–[a]	0.010	–[a]	–[a]	0.004

[a] kinetic phase not present.

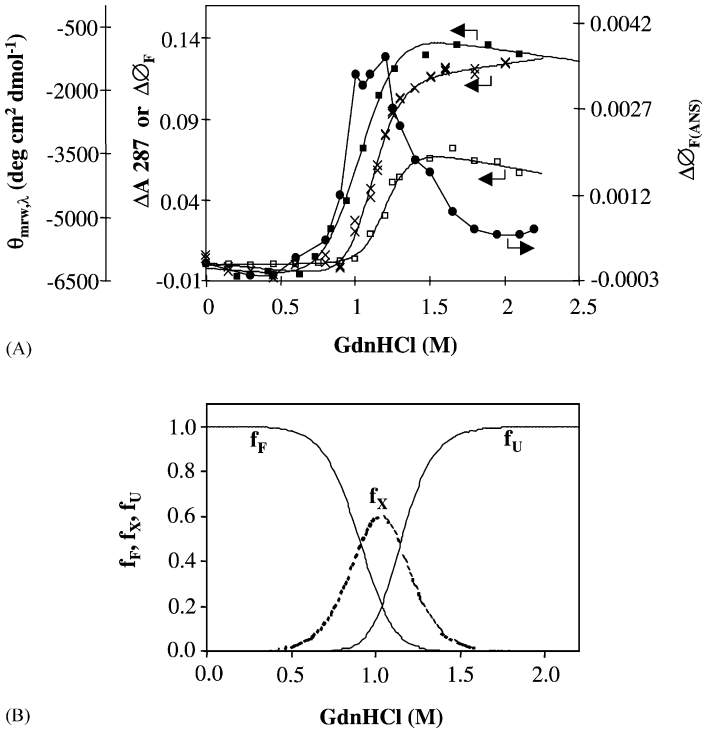

Fig. 4. Unfolding of cutinase at pH 4.5 induced by guanidine hydrochloride. (A) Transition curves were followed by near-UV difference spectroscopy at 287 nm (■), cutinase fluorescence (□) ANS fluorescence (●) and mean residue ellipticity at 222 nm (⊗). Solid lines fit unfolding curves according to Staniforth et al. [33], except for ANS fluorescence. (B) Accumulation of the intermediate calculated according to Staniforth et al. [33].

absorbance and tryptophyl fluorescence to probe tertiary structure and by far-UV circular dichroism to probe secondary structure [20]. The transitions followed by different techniques were non-coincidental occurring at different guanidine hydrochloride concentrations (Fig. 4A). It is worth noticing that the UV absorbance at 287 nm (at this wavelength the UV difference absorbance is mainly due to the exposure of tyrosine residues [31]) changes before tryptophyl fluorescence intensity (excited selectively at 296 nm). This non-coincidence of the curves is the diagnostic for the presence of at least one stable intermediate within the transition region [32] and the data was fitted according to a three-state process (F ↔ X ↔ U) using the model proposed by Staniforth et al. [20,33]. The mid-points for the transitions are shown in Table 3 and the accumulation of the intermediate is shown in Fig. 4B. In order to characterize the intermediate, the unfolding transition was also followed by ANS fluorescence intensity (Fig. 4A). The fluorescence of ANS increases when the intermediate is present, showing its molten globule character. Molten globule intermediates: (1) are condensed in a globular form; (2) contain native-like secondary structure; (3) are stabilised mainly by non-specific hydrophobic interactions; (4) have a topology close to the native state; and (5) are “molten” in character [28]. The intermediate conformation of cutinase shares some of these characteristics (Table 3). The secondary structure is native-like as shown by the mean residue ellipticity at 222 nm (-6000° cm^2 dmol^{-1}) which is close to that of folded state. Many tertiary interactions of the folded state were lost including those surrounding the tyrosyl microenvironment. These interactions were probed by the near-UV difference absorbance at 287 nm which changed by around 70% in the absence of trehalose [20]. The intermediate is close to the folded state in terms of space-neighbouring

Table 3
Parameters for cutinase unfolding at pH 4.5 induced by guanidine hydrochloride according to a three-state process [33]

	$[GdnHCl_{50\%,1}]$[a] (M)	$[GdnHCl_{50\%,2}]$[a] (M)	n_1[b]	n_2[b]	I_X[c]
No solute					
ΔA	0.98 ± 0.15	1.21 ± 0.02	52	66	0.104
$\Delta\phi_F$	1.11 ± 0.00	1.18 ± 0.11	50	68	0.007
$[\theta]_{mrw,\lambda}$	0.92	1.11	52	67	−6000
0.5 M trehalose					
ΔA	1.29 ± 0.02	1.40 ± 0.02	52	66	0.065
$\Delta\phi_F$	1.41 ± 0.07	1.39 ± 0.07	52	67	0.006

Transitions were assessed by near-UV difference spectroscopy at 287 nm (ΔA), tryptophyl fluorescence quantum yields difference ($\Delta\phi_F$) and mean residue ellipticity at 222 nm ($[\theta]_{mrw,\lambda}$).

[a] Guanidine hydrochloride concentration required to achieve 50% of the first or second transition, respectively.

[b] Total of side-chains becoming exposed during the first or second transition, respectively. The "what–if" program [34] and the atomic co-ordinates of *F. solani* cutinase (PDB entry 1AGY) were used to calculate the fraction of amino acid side-chains buried in the folded state in comparison to a fully extended conformation [20].

[c] Near-UV absorbance difference, tryptophyl quantum yield difference or mean residue ellipticity ($^\circ$ cm^2 dmol^{-1}) at 222 nm of the intermediate.

residues. This conclusion could be drawn as the single tryptophan residue of cutinase (in position 69) is strongly quenched by the neighbouring disulfide bond (between cysteines 31 and 109) in the folded conformation and remains quenched in the intermediate since the fluorescence intensity for the intermediate changes by only 10%. These equilibrium intermediates seem to be analogues to the folding intermediates detectable by conventional kinetic methods [35] pointing to their importance as productive intermediates in the pathway towards the folded state.

As we have observed for the thermal unfolding, trehalose does not change the unfolding pathway as indicated by the nature of the intermediate present at equilibrium. The number of side-chains exposed on the intermediate is not different in the presence of trehalose (Table 3). Only the mid-points were shifted to higher guanidine hydrochloride concentrations showing the stabilisation effect of trehalose on both transitions [20].

3. Cutinase stability in AOT reverse micelles: the effect of 1-hexanol

The encapsulation of cutinase in AOT reverse micelles induces a time-dependent unfolding process at room temperature characterised by fluorescence and activity measurements [36]. The unfolding is clearly identified when the fluorescence emission spectra of cutinase in AOT reverse micelles is compared to the spectra in aqueous solution and of thermally unfolded cutinase (Fig. 5). The emission peak of cutinase in aqueous solution occurs at 303 nm when both tyrosine and tryptophan residues are excited (excitation at 280 nm). The emission peak in the range of free tyrosine along with decomposition of the spectrum at tryptophan and tyrosine contributions shows that emission is dominated by tyrosyl residues. After

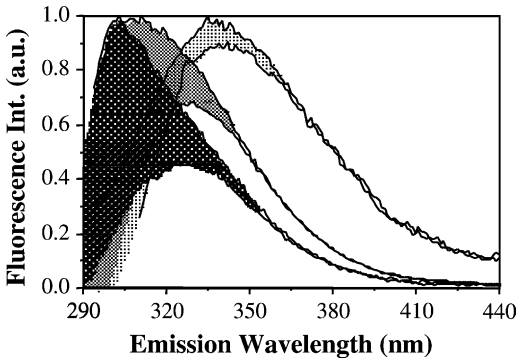

Fig. 5. Fluorescence emission spectra of cutinase in aqueous solution (darker spectrum), encapsulated in reverse micelles of AOT (spectrum filled with an intermediate pattern) and thermal unfolded (brighter spectrum). The filled areas are the contribution of tyrosine residues to total emission and the empty areas under the filled ones are the emission of the single tryptophan residue, calculated as described in [36].

thermal unfolding, the spectra became dominated by tryptophyl emission with the maximum occurring at 335 nm. The emission spectrum of cutinase encapsulated in AOT reverse micelles is clearly approaching that obtained for unfolded cutinase. It shows a larger contribution from tryptophyl to total emission, although less significant than that for unfolded cutinase, causing a red shift of the peak from 303 to 311 nm.

Cutinase unfolding in AOT reverse micelles is coupled to deactivation [23]. Both functional stability assessed by the time-dependent loss of activity and structural stability assessed by the time-dependent fluorescence intensity changes show the same trend with time (Fig. 6). The kinetics of the unfolding of cutinase in AOT reverse micelles depend on the size of the reverse micelle being faster at larger reverse micelles. The size is usually defined in terms of the parameter W_0 which is the ratio of molarity of water to molarity of surfactant and can be changed with a concomitant change on the properties of the water inside the reverse micelle [37].

Dynamic light scattering was used to resolve two populations of reverse micelles, one empty and the other filled with cutinase, as long as the two populations have significantly different radii [24]. If the unfolding kinetics were slow, a decrease on the water pool radius was observed for reverse micelles filled with cutinase. This indicates that cutinase is attached to the micellar interface inducing an increase of the interfacial area and a decrease of the water pool radius. This location might cause the unfolding of cutinase. The interactions between cutinase and the AOT interface are probably the driving force to unfold cutinase at room temperature. The denaturation effect of negatively charged surfactants is well documented, namely for cutinase [38]. Attempts to increase the stability of cutinase in AOT reverse micelles were based on a factorial design study [15]. Two parameters were identified as being critical with respect to increasing the stability: the size of the reverse micelle and the concentration of 1-hexanol which acts as co-surfactant being located between the AOT molecules as part of the reverse micellar interface. Actually, 1-hexanol is a co-surfactant and a substrate for esterification reactions. Optimal stabilities were achieved at W_0 2.7 and 0.4 M of hexanol leading to half-life times of 53 days at 30 °C. The presence of hexanol as co-surfactant changes the interfacial properties of the reverse micelle and a new equilibrium is established. One AOT/hexanol reverse micelle filled with cutinase is built up with one cutinase molecule and the fusion of several empty reverse micelles to give a reverse micelle about 10-fold larger [25]. Encapsulation of cutinase in this large reverse micelle prevents denaturation. The two situations in the absence and presence of hexanol are clearly distinct with respect to the size of the reverse micelle filled with cutinase. The radius of the filled reverse micelle in the presence of hexanol can be as large as 100 nm compared to less than 12 nm for a filled reverse micelle in the absence of hexanol [25]. This effect is the opposite of the effect on empty reverse micelles as hexanol decreases the size of empty reverse micelles. The operational stability of cutinase in the AOT/hexanol system is also highly improved leading to an estimated operational half-life of 674 days under continuous operation in a membrane bioreactor [39]. Therefore, the disadvantage of low enzyme stabilities sometimes observed with non-conventional media such as cutinase in AOT reverse micelles can be altered to more favourable cases.

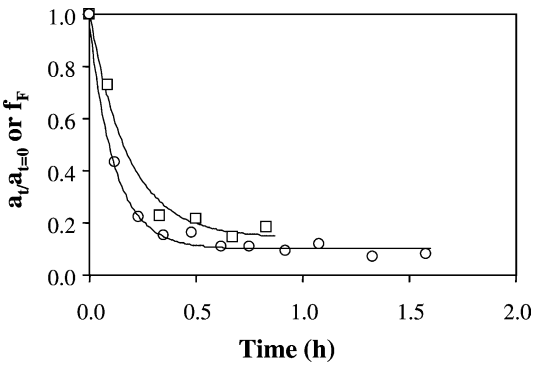

Fig. 6. Functional and structural stability of cutinase in AOT reverse micelles at W_0 20. Functional stability was assessed by the loss of activity, $a_t/a_{t=0}$ (□) and structural stability was assessed by the fraction of cutinase molecules in the folded state (○) calculated according to: $f_F = (FI_{330(t=1.85\,h)} - FI_{330(t)})/(FI_{330(t=1.85\,h)} - FI_{330(t=0\,h)})$, where FI_{330} is the fluorescence intensity at 330 nm at time t. After 1.85 h, cutinase was assumed to be unfolded. The solid lines fit a first-order process with rate constants of 5.7 and 8.4 h^{-1} for functional and structural stability, respectively. The difference between the rate constants is not significant considering the number of data points collected during the decay.

Acknowledgements

We thank Dr. Daniel Graham for the English revision. Financial support from Fundação para a Ciência e Tecnologia, Portugal, contract Praxis/C/BIO/14314/1998 is acknowledged.

References

[1] P.E. Kolattukudy, in: B. Borgström, H.L. Brockman (Eds.), Lipases, Elsevier, New York, 1984, Chapter IIIC, p. 471.
[2] M. Lauwereys, P. De Geus, J. De Meutter, P. Stanssens, G. Mathyssens, in: L. Alberghina, R.D. Schmid, R. Verger (Eds.), Lipases—Structure, Function and Genetic Engineering, VCH, Weinheim, 1991, p. 243.
[3] U. Derewenda, L. Swenson, R. Green, Y. Wei, S. Yamaguchi, R. Joerger, M.J. Haas, Z.S. Derewenda, Protein Eng. 7 (1994) 551.
[4] C. Martinez, Structure cristalline a 1.6 Å de resolution d'une cutinase recombinant de *Fusarium solani pisi*, Ph.D. Thesis, Universite de Paris-Sud, Paris, 1992.
[5] M.R. Egmond, C.J. van Bemmel, Methods Enzymol. 284 (1997) 119.
[6] H. van Tilbeurgh, M.P. Egloff, C. Martinez, N. Rugani, R. Verger, C. Cambillau, Nature 362 (1993) 814.
[7] C. Martinez, P. de Geus, M. Lauwereys, G. Matthyssens, C. Cambillau, Nature 356 (1992) 615.
[8] S. Longhi, M. Czjzek, V. Lamzin, A. Nicolas, C. Cambillau, J. Mol. Biol. 268 (1997) 779.
[9] J.J. Prompers, B. van Noorloos, M.L. Mannesse, A. Groenewegen, M.R. Egmond, H.M. Verheij, C.W. Hilbers, H.A. Pepermans, Biochemistry 38 (1999) 5982.
[10] M.L.M. Mannesse, R.C. Cox, B.C. Koops, H.M. Verheij, G.H. de Haas, M.R. Egmond, H.T.W.M. van der Hijden, J. de Vlieg, Biochemistry 34 (1995) 6400.
[11] Genencor, Increasing pharmacological effect of agricultural chemicals, US Patent 88,08945 (1988).
[12] J.A.C. Flipsen, A.C.M. Appel, H.T.W.M. van der Hijden, C.T. Verrips, Enzyme Microb. Technol. 23 (1998) 274.
[13] Unilever, Enzyme-containing surfactant compositions, US Patent 94,04771 (1994).
[14] C.A. Murphy, J.A. Cameron, S.J. Huang, R.T. Vinopal, Appl. Environ. Microbiol. 62 (1996) 456.
[15] C.M.L. Carvalho, J.M.S. Cabral, M.R. Aires-Barros, Enzyme Microb. Technol. 24 (1999) 569.
[16] V.V. Mozahev, Trends Biotechnol. 11 (1993) 88.
[17] A.M. Klibanov, T.J. Ahern, in: D.L. Oxender, C.F. Fox (Eds.), Protein Engineering, Alan R. Liss Inc., New York, 1987, Chapter 19, p. 213.
[18] P.X. Qi, T.R. Sosnick, S.W. Englander, Nat. Struct. Biol. 5 (1998) 882.
[19] R.P. Baptista, J.M.S. Cabral, E.P. Melo, Biotechnol. Bioeng. 70 (2000) 699.
[20] E.P. Melo, T.Q. Faria, L.O. Martins, A.M. Gonçalves, J.M.S. Cabral, Proteins 42 (2001) 542.
[21] S.N. Timasheff, in: B.A. Shirley (Ed.), Protein Stability and Folding: Theory and Practice, Humana Press, Totowa, NJ, 1995, p. 253.
[22] J.F. Back, D. Oakenfull, M.B. Smith, Biochemistry 18 (1979) 5191.
[23] E.P. Melo, C.M.L. Carvalho, M.R. Aires-Barros, S.M.B. Costa, J.M.S. Cabral, Biotechnol. Bioeng. 58 (1998) 380.
[24] E.P. Melo, P. Fojan, J.M.S. Cabral, S.B. Petersen, Chem. Phys. Lipids 106 (2000) 181.
[25] E.P. Melo, S.M.B. Costa, J.M.S. Cabral, P. Fojan, S.B. Petersen, Chem. Phys. Lipids (2003) in press.
[26] E.P. Melo, M.R. Aires-Barros, S.M.B. Costa, J.M.S. Cabral, J. Biochem. Biophys. Methods 34 (1997) 45.
[27] B. Fischer, I. Sumner, P. Goodenough, Arch. Biochem. Biophys. 306 (1993) 183.
[28] H. Christensen, R.H. Pain, in: R.H. Pain (Ed.), Mechanisms of Protein Folding, Oxford University Press, Oxford, 1994, Chapter 3, p. 55.
[29] D.B. Volkin, A.M. Klibanov, in: T.E. Creighton (Ed.), Protein Function: A Practical Approach, IRL Press, Oxford, 1989, p. 213.
[30] S.E. Zale, A.M. Klibanov, Biotechnol. Bioeng. 15 (1983) 2221.
[31] F.X. Schmid, in: T.E. Creighton (Ed.), Protein Structure: A Practical Approach, IRL Press, Oxford, 1989, p. 251.
[32] C.N. Pace, Methods Enzymol. 131 (1986) 266.
[33] R.A. Staniforth, S.G. Burston, C.J. Smith, G.S. Jackson, I.G. Badcoe, T. Atkinson, J.J. Holbrook, A.R. Clarke, Biochemistry 32 (1993) 3842.
[34] G. Vriend, J. Mol. Graph. 8 (1990) 52.
[35] H. Roder, W. Colón, Curr. Opin. Struct. Biol. 7 (1997) 15.
[36] E.P. Melo, S.M.B. Costa, J.M.S. Cabral, Photochem. Photobiol. 63 (1996) 169.
[37] P.L. Luisi, M. Giomini, M.P. Pileni, B.H. Robinson, Biochem. Biophys. Acta 947 (1988) 209.
[38] D.J. Pocalyko, M. Tallman, Enzyme Microb. Technol. 22 (1998) 647.
[39] C.M.L. Carvalho, M.R. Aires-Barros, J.M.S. Cabral, Biotechnol. Bioeng. 72 (2000) 127.